

An electron microscopy study of the effect of Ce on plasma sprayed bronze coatings

This article has been downloaded from IOPscience. Please scroll down to see the full text article.

2012 J. Phys.: Conf. Ser. 371 012085

(<http://iopscience.iop.org/1742-6596/371/1/012085>)

View [the table of contents for this issue](#), or go to the [journal homepage](#) for more

Download details:

IP Address: 152.78.178.43

The article was downloaded on 02/10/2012 at 19:01

Please note that [terms and conditions apply](#).

An electron microscopy study of the effect of Ce on plasma sprayed bronze coatings

Li Wensheng¹, S.C. Wang², Chao Ma², Wang Zhiping¹

1. State Key Laboratory of Advanced Nonferrous Materials, Lanzhou University of Technology, Lanzhou, 730050, China

2. National Centre for Advanced Tribology at Southampton, School of Engineering Sciences, University of Southampton, SO17 1BJ, United Kingdom

Abstract: The Cu-Al eutectoid alloy is an excellent material for mould due to its superior low friction. The conventional sand casting technique, however, is not feasible to fabricate high Al bronze because of high hardness and brittleness. Plasma arc spray has been used to produce high Al/Fe bronze coatings for mould. The inherent impurities such as H, O, N, S during the spray, however, may affect the coating's mechanical strength. One approach is to utilise the active rare earth Ce to clean up these impurities. The study is to investigate the effect of Ce on the microstructure, which has few reported in the literature.

1. Introduction

The copper based aluminium (5-12 wt.%) bronzes possess low wear rate and coefficient of friction, and have been widely used for tool, gears, bearings, valves, propellers especially on drawing and rolling die industry. Their hardness, which is between 190-240 HB, is not high enough to make a more precision die finish. Therefore, new interest has been raised on aluminum bronze with Al contents over 12 wt.% with the hardness at 400 HB [1,2]. Fe was also added in aluminum bronzes to enhance the corrosion resistance as long as the iron remains in solution and not precipitated as pure iron [3]. Since the conventional sand casting techniques are not feasible to fabricate Al/Fe bronze over the equilibrium solubilities (9.4 wt.% Al and 3.5 wt% Fe), thermally plasma spray has been attempted to make a saturated Cu-14Al-4.5Fe (wt.%) copper-aluminum-iron coating. As the unavoidable impurities such as H, O, N, S will affect the coating's mechanical strength especially the interface adhesion strength, the rare earth Ce has been added to clean up these impurities. The paper aims to study the Ce effect on the coating microstructure. Our previous study [4] showed the possible intermetallics, as listed in Table 1. Due to the lattice similarity among these phases, X-ray diffraction was found difficult to identify the structures. Transmission electron microscopy (TEM) is therefore used to investigate the microstructure with and without Ce, in order to understand the effect of Ce on the microstructure and properties.

Table 1 Characteristics of the equilibrium phases in aluminum bronze

| Phases | Crystal Structure | Lattice Spacing | Micro-Hardness (HV) |
|---|----------------------------------|-----------------|---------------------|
| α (Cu) | A1 (Fm $\bar{3}$ m) | 0.364 nm | 200-270 |
| γ_2 (Cu ₉ Al ₄) | D8 ₃ (P $\bar{4}$ 3m) | 0.869 nm | 360-570 |
| β' (Cu ₃ Al) | L12 (Pm $\bar{3}$ m) | 0.353 nm | 290-407 |
| κ_1 (Fe ₃ Al) | DO ₃ (Fm $\bar{3}$ m) | 0.571 nm | >700 |
| κ_2 (FeAl) | B2 (Pm $\bar{3}$ m) | 0.29 nm | >650 |

2. Experimental

The Cu-Al-Fe alloys with free Ce and 0.6 wt.% Ce respectively were melted at 1200°C ~ 1260°C, followed by water cooling atomization to form the alloys powders with the compositions listed in Table 2. These powders were then plasma sprayed thermally on mild steel. The detail was reported in ref [4]. Rockwell hardness was tested on the HD1-187.5 sclera-meter with a load of 150 Kg. The specimens were etched using a solution consisting of 5 g FeCl₃, 10 ml HCl and 100 ml distilled water. The image observation and element mapping were performed in scanning electron microscope (SEM) JSM6500F and EPMA-1610 Electronic Probe Microanalysis equipped with an OXFORD ISIS 300 EDS analyzer. The TEM specimens were prepared using electro-polishing solution of 20% HNO₃, 15% 2-butoxyethanol and 65% methanol in volume, and JEM3010 at 300 kV was used for analysis.

Table 2 Chemical composition of Cu-14Al-4.5Fe alloy

| Ingredients | Cu | Al | Fe | Co | Ni | Others |
|--------------------|-------|-------|-------|---------|---------|---------|
| Weight percent (%) | 75-80 | 13-16 | 2-4.5 | 0.5-0.8 | 0.4-0.6 | 1.0-2.6 |

3. Results and Discussion

The Ce-free coating consists of inhomogenous intermetallics ranged from a few to tens of microns, as shown by backscattered electron (BSE) image in Fig.1. These intermetallics show dark contrast in the element map of Cu, the bright contrast in the element map of Fe and grey colour in the element map of Al. It indicates that they are most likely κ_2 (FeAl). It is also interesting that the intermetallics in the element map of Fe appear larger than those in the element map of Cu, as compared in the same area (e.g. highlighted circle). The high magnified color image in the insert of Cu map shows clearly that a thin layer surrounds the κ_2 phase. The composition is close to γ_2 (Cu₉Al₄) with Iron rich.

In contrast, the Ce added coating has more homogenous intermetallics at roughly 10 μ m as shown in Fig. 2. Again the intermetallics in the element map of Fe are larger than those in the element map of Cu. These intermetallics have the dominating κ_1 (Fe₃Al) and γ_2 (Cu₉Al₄) with Fe rich. Figs. 3 & 4 show the magnified secondary electron (SE) images in the rectangular areas of Figs. 1 & 2, respectively. Two coatings have shown the different microstructures: for Ce-free coating, EDS confirm that there exist large γ_2 intermetallics (position 1 in Fig. 3), and a number of small dispersoid particles κ_2 (position 2, in a diameter of a few hundred nanometre). The high concentration of Cu in κ_2 phase is due to the contribution from the matrix β' (Cu₃Al). For Ce-added coating, the matrix β' zones are precipitates free (Fig. 4), and the κ_1 and γ_2 particles seem to coexist in “boat” shaped areas (Position 2 & 3).

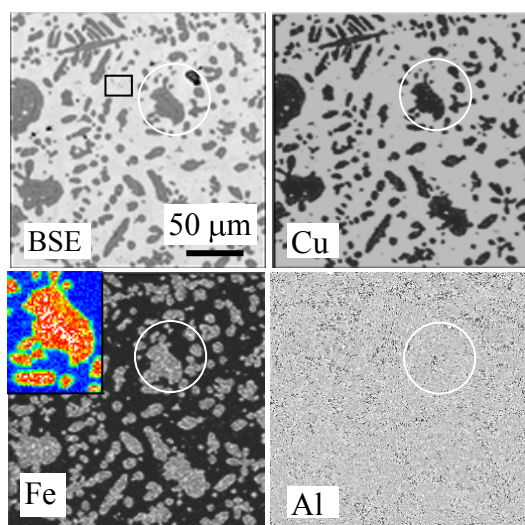


Fig.1 BSE image and element maps of Cu, Fe & Al of the Ce-free coating

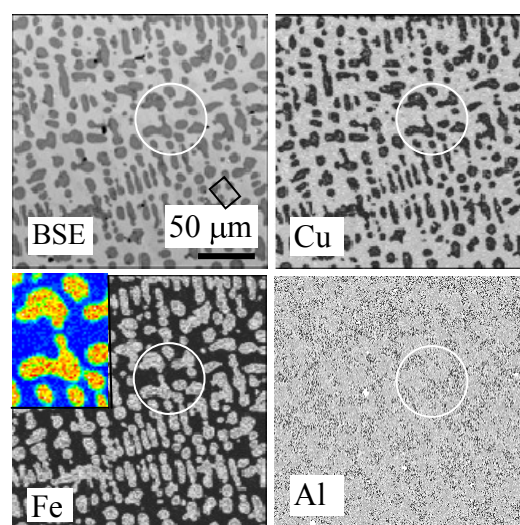


Fig.2 BSE image and element maps of Cu, Fe & Al of the Ce-added coating



Fig.3 Magnified SE image on the Ce-free coating

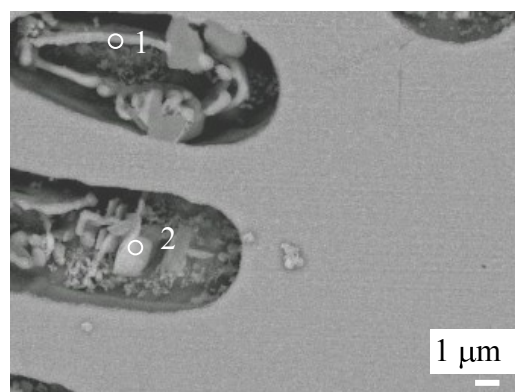


Fig.4 Magnified SE image on the Ce-added coating

| Position | Al(at.%) | Fe(at.%) | Cu(at.%) | Phase | Position | Al(at.%) | Fe(at.%) | Cu(at.%) | Phase |
|----------|----------|----------|----------|------------------------------------|----------|----------|----------|----------|------------------------------------|
| 1 | 16.3 | 6.8 | 76.9 | $\gamma_2(\text{Cu}_9\text{Al}_4)$ | 1 | 17.5 | 6.8 | 75.7 | $\gamma_2(\text{Cu}_9\text{Al}_4)$ |
| 2 | 16.7 | 22.6 | 60.7 | $\kappa_2(\text{FeAl})$ | 2 | 20.0 | 63.5 | 16.5 | $\kappa_1(\text{Fe}_3\text{Al})$ |

EDS in SEM could be used for the preliminary work on phase identification via composition, but it could be uncertain without diffraction analysis. TEM has therefore been used for the structure determination. The bright field (BF) of the Ce-free coating in Fig. 5a shows the round dispersoid at a hundred nanometres. The corresponding diffraction pattern in Fig. 5b to position 1 in Fig. 5a confirms the matrix indeed as $\beta'(\text{Cu}_3\text{Al})$. The very fine grey particles (~ten nanometers) are the artifact caused by the eletropolish. The dispersoid (position 2 in Fig. 5a) has been determined as $\kappa_2(\text{FeAl})$ as indexed in Fig. 5c (some extra spots come from the matrix). For Ce-added coating, the matrix has again $\beta'(\text{Cu}_3\text{Al})$ indexed in Fig. 6b for Position 1 of Fig. 6a. The micron-sized $\kappa_1(\text{Fe}_3\text{Al})$ phase has been confirmed in Fig. 6c for Position 2 of Fig. 6a. The different structure of the Fe-containing intermetallics could result in different hardness on coatings (Table 1). In addition, stacking faults have been observed with Ce coating as shown in Fig. 6d. It indicates that the addition of Ce has reduced the stacking fault energy (SFE). It has been reported that the wear rate would be decreased with the decrease of SFE in Cu-Al alloy [5]. This observation is

consistent to our tribological results that the coatings with Ce has reduced the wear rate by 10%, and enhanced the strengthening by 10% [4].

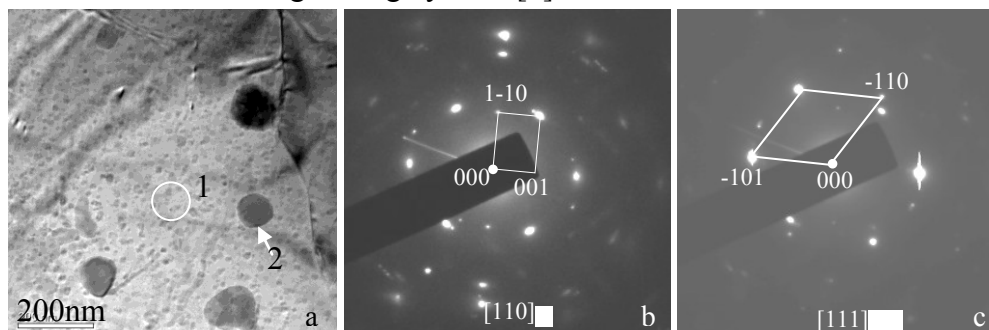


Fig. 5 TEM BF image (a) of Ce-free coating. The diffraction patterns in Figs. 5b & 5c corresponding to Positions 1 & 2, respectively.

| Position | Al(at.%) | Fe(at.%) | Cu(at.%) | Mn(at.%) | Co(at.%) | Ni(at.%) | Phase |
|----------|----------|----------|----------|----------|----------|----------|-------------------------------------|
| 1 | 19.3 | 2.8 | 77.9 | - | - | - | β' (Cu_3Al) |
| 2 | 24.1 | 15.2 | 44.4 | 1.1 | 3.1 | 12.0 | κ_2 (FeAl) |

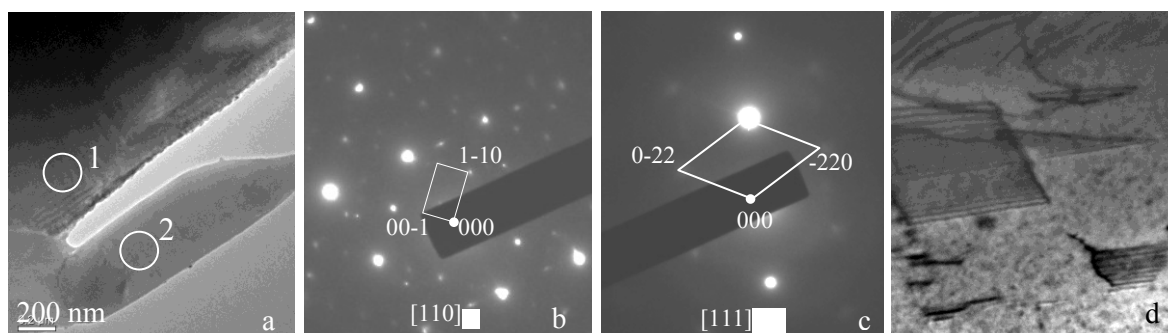


Fig. 6 TEM BF images (a, d) of Ce-added coating. The diffraction patterns in Figs. 6b & 6c corresponding to Positions 1 & 2, respectively.

| Position | Al(at.%) | Fe(at.%) | Cu(at.%) | Mn(at.%) | Phase |
|----------|----------|----------|----------|----------|---------------------------------------|
| 1 | 23.4 | 1.9 | 73.8 | 0.83 | β' (Cu_3Al) |
| 2 | 21.3 | 69.2 | 8.2 | 1.3 | κ_1 (Fe_3Al) |

4. Conclusions

The effect of Ce addition on the microstructure of thermally plasma spray coatings was studied by electron microscopy. For Ce-free coating, the intermetallics were κ_2 (FeAl) surrounding by γ_2 (Cu_9Al_4) with Fe rich phase. In contrast, κ_1 (Fe_3Al) were dominating intermetallics in Ce-added coating. This indicates that Ce stimulates the transition of the Fe-containing intermetallics from FeAl to Fe_3Al . Stacking faults were also observed in the coating with Ce addition, which is responsible for the reduced wear rate and increase of the strengthening.

References

- [1] Heide E, Stam ED, Girand H, Lovato G, Akdut N, et al, 2006 *Wear* **261** 68-73
- [2] Li WS, Wang ZP, Lu Y, Jin YH, Yuan LH, Wang F 2006 *Wear* **261** 155-163
- [3] Moreton BB 1985 *Corr. Prev. Control* **6** 122-126
- [4] Li WS, Lu Y, Yuan K, and Yuan C 2011 *Journal of Rare Earths* **29** 363
- [5] Wert JJ and William MC 1988 *Wear* **123** 171